DALTON

Synthesis, molecular and electronic structure of Ru_3 isomeric clusters carrying C_8 rings bonded in allenylic and acetylenic modes†

Dario Braga,*[a] Fabrizia Grepioni,[a] David B. Brown,[b] Brian F. G. Johnson,*[b] Maria J. Calhorda*[c] and Luis F. Veiros[d]

[a] *Dipartimento di Chimica G. Ciamician, Università di Bologna, Via Selmi 2, 40126 Bologna, Italy*
[b] *Chemical Laboratory, The University of Cambridge, Lensfield Road, Cambridge CB2 1EW, UK*
[c] *ITQB, R. da Quinta Grande, 6, Apart. 127, 2780 Oeiras and IST, Lisboa, Portugal*
[d] *Centro de Química Estrutural, IST, Av. Rovisco Pais, 1096 Lisboa Codex, Portugal*

The two new cluster complexes $[Ru_3H_2(CO)_9(C_8H_{10})]$ **1** and $[Ru_3H(CO)_9(C_8H_{11})]$ **2** have been isolated as the products of thermolysis of $[Ru_3(CO)_{12}]$ in octane containing cycloocta-1,3-diene. The two species are structural isomers ideally differing only in the transfer of one hydrogen atom from the organic ligand to the metal core. The organic ligand in **2** is bonded in an allenyl μ_3-η^3 fashion, the first allenylic bonded ring system to have been reported, whereas in **1** the ligand is, more conventionally, bound in μ_3-η^2 fashion with the second unsaturated C=C bond not involved in bonding to the cluster. The solid-state structures of **1** and **2** have been studied by single-crystal X-ray diffraction. The bonding of the organic ligands in the clusters has been investigated by molecular orbital calculations of the extended-Hückel type.

Transition-metal clusters containing the allenyl ligand have been synthesized by reaction of transition-metal prop-2-ynyl complexes with carbonyl clusters which yield bi- and tri-nuclear compounds containing the allenyl unit,[1] and by the coupling of two separate hydrocarbon units.[2] The first allenyl cluster compound to be reported[3] was $[Ru_3(CO)_9(\mu_3\text{-}\eta^1\text{:}\eta^1\text{:}\eta^2\text{-}C_6H_9)]$ obtained from the thermolysis of $[Ru_3(CO)_{12}]$ with *cis*- and *trans*-hexa-1,3-diene in benzene; it appears to be the only transition-metal cluster containing an allenyl unit synthesized *via* a thermolysis.

In this paper we report on the synthesis of a cluster in which an allenylic unit is bonded to a ruthenium unit derived from the reaction of cycloocta-1,3-diene with $[Ru_3(CO)_{12}]$. The thermolysis of $[Ru_3(CO)_{12}]$ in octane containing cycloocta-1,3-diene affords a range of products in varying yields; we concentrated on two novel triruthenium hydride complexes, *viz*. $[Ru_3H_2(CO)_9(\mu_3\text{-}\eta^2\text{-}C_8H_{10})]$ **1** and $[Ru_3H(CO)_9(\mu_3\text{-}\eta^3\text{-}C_8H_{11})]$ **2**, which have been isolated and fully characterized by single-crystal X-ray diffraction methods. We also discuss the bonding in the two species by means of molecular orbital calculations of the extended-Hückel type.

Results and Discussion

Synthesis and structural characterization of complexes 1 and 2

The thermolysis of $[Ru_3(CO)_{12}]$ in octane containing cycloocta-1,3-diene affords a range of products in varying yields, two of which have been isolated and identified as $[Ru_3H_2(CO)_9(\mu_3\text{-}\eta^2\text{-}C_8H_{10})]$ **1** and $[Ru_3H(CO)_9(\mu_3\text{-}\eta^3\text{-}C_8H_{11})]$ **2**. Single-crystal X-ray diffraction experiments show that both compounds consist of a triangular ruthenium framework with three carbonyls bonded to each ruthenium. Relevant structural parameters are reported in Tables 1 and 2, for species **1** and **2**, respectively.

The asymmetric unit of crystalline complex **1** contains two independent molecules (**1a** and **1b**) which differ in the hydride location and in the folding of the outer aliphatic chain of the C_8H_{10} ligand [see Fig. 1(*a*) and 1(*b*)]. The organic ligand in **1** is bound to the cluster *via* two σ and one π interaction in an alkyne fashion seen before for many linear and ring systems.[4] The free olefinic bond does not interact with the metal atoms of the cluster. Possible hydride-atom positions, calculated using XHYDEX[5] (see Table 3), were found along the Ru(1)–Ru(3), and Ru(2)–Ru(3) edges in **1a** [see Fig. 2(*a*) and 2(*b*)] and along the Ru(4)–Ru(6) and Ru(5)–Ru(6) edges in **1b** as well as on the face of the cluster for both independent molecules [see Fig. 3(*c*)

Table 1 Selected bond lengths (Å) and angles (°) for complex **1** (molecules **1a** and **1b**)

1a		**1b**	
Ru(1)–Ru(2)	2.730(2)	Ru(5)–Ru(6)	2.727(2)
Ru(1)–Ru(3)	2.824(2)	Ru(5)–Ru(4)	3.010(2)
Ru(2)–Ru(3)	2.998(2)	Ru(6)–Ru(4)	2.844(2)
Ru(1)–C(10)	2.283(9)	Ru(5)–C(27)	2.081(8)
Ru(2)–C(10)	2.087(8)	Ru(6)–C(27)	2.284(8)
Ru(1)–C(11)	2.252(8)	Ru(4)–C(28)	2.126(8)
Ru(3)–C(11)	2.118(8)	Ru(6)–C(28)	2.230(8)
C(10)–C(11)	1.37(1)	C(27)–C(28)	1.37(1)
C(10)–C(17)	1.52(1)	C(27)–C(34)	1.51(1)
C(11)–C(12)	1.48(1)	C(28)–C(29)	1.49(1)
C(12)–C(13)	1.32(2)	C(29)–C(30)	1.34(1)
C(13)–C(14A)	1.58(2)	C(30)–C(31)	1.51(1)
C(13)–C(14B)	1.33(3)	C(31)–C(32)	1.50(1)
C(14A)–C(15A)	1.56(2)	C(32)–C(33)	1.53(1)
C(14B)–C(15B)	1.50(4)	C(33)–C(34)	1.52(1)
C(15A)–C(16)	1.49(2)		
C(15B)–C(16)	1.71(3)		
C(16)–C(17)	1.52(1)		
Ru–C (CO) mean	1.931(10)		1.931(10)
C–O (CO) mean	1.13(1)		1.13(1)
C(11)–C(10)–C(17)	123(1)	C(28)–C(27)–C(34)	122(1)
C(10)–C(11)–C(12)	124(1)	C(27)–C(28)–C(29)	126(1)
C(13)–C(12)–C(11)	123(1)	C(30)–C(29)–C(28)	130(1)
C(12)–C(13)–C(14B)	142(2)	C(29)–C(30)–C(31)	132(1)
C(12)–C(13)–C(14A)	122(1)	C(32)–C(31)–C(30)	120(1)
C(15A)–C(14A)–C(13)	112(1)	C(31)–C(32)–C(33)	115(1)
C(16)–C(15A)–C(14A)	112(1)	C(34)–C(33)–C(32)	114(1)
C(15B)–C(14B)–C(13)	116(3)	C(27)–C(34)–C(33)	110(1)
C(14B)–C(15B)–C(16)	113(2)		
C(15A)–C(16)–C(17)	117(1)		
C(17)–C(16)–C(15B)	109(1)		
C(10)–C(17)–C(16)	114(1)		

† *Non-SI units employed*: eV ≈ 1.60 × 10^{-19} J, cal = 4.184 J.

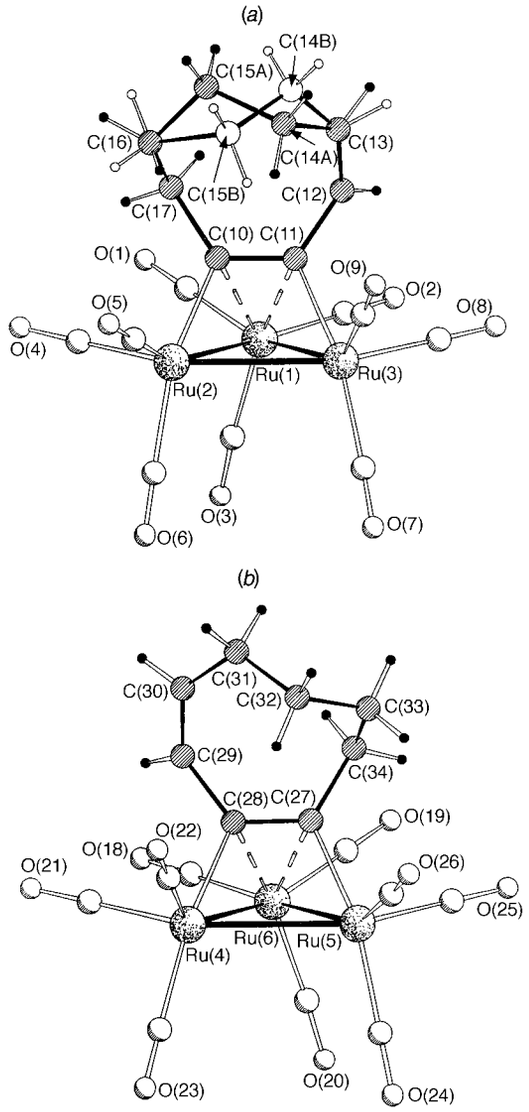

Fig. 1 Solid-state molecular structures of molecules **1a** (*a*) and **1b** (*b*) showing the atomic labelling schemes. Molecule **1a** is disordered with atoms C(14) and C(15) occupying two sites of occupancy 60 and 40%

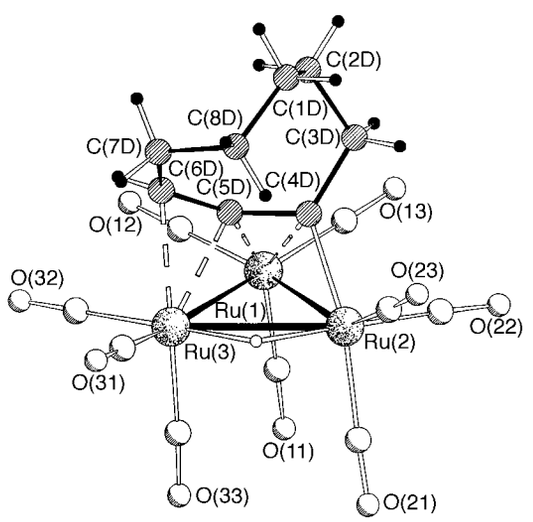

Fig. 2 Solid-state molecular structure of complex **2** showing the atomic labelling scheme

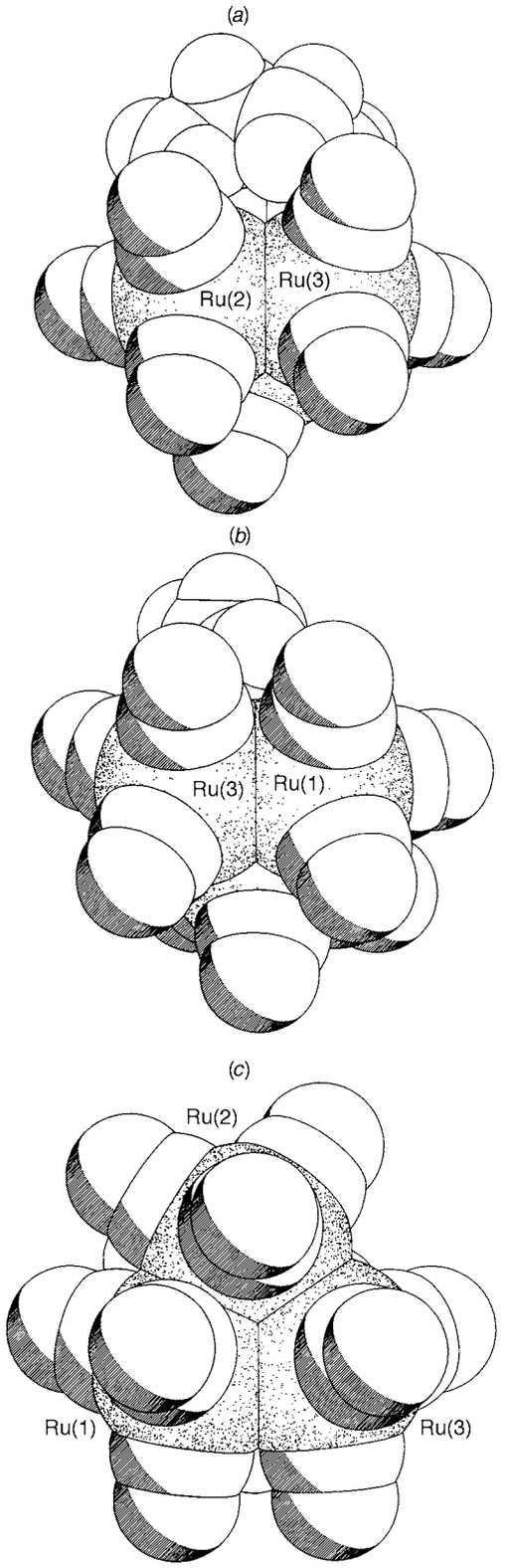

Fig. 3 Space-filling diagrams showing carbonyl displacement around supposed hydride positions: edges Ru(1)–Ru(3) (*b*) and Ru(2)–Ru(3) (*a*) and face Ru(1)–Ru(2)–Ru(3) (*c*) for molecule **1a**

in the case of **1a**]. These results were compared with those obtained from low-θ Fourier-difference scans ($2\theta < 40°$). While in **1a** suitable H-atom positions were found at the centre of the triangle face [Ru(1)-H 1.678, Ru(2)-H 1.908, Ru(3)-H 1.671 Å] and along the Ru(1)–Ru(3) edge [Ru(1)-H 1.746, Ru(3)-H 1.887 Å] in agreement with the XHYDEX results, in **1b** a disordered distribution of the two H over the edge-bridging positions was observed. The solution ^{1}H NMR spectrum shows a broad sing-

Table 2 Selected bond lengths (Å) and angles (°) for complex **2**

Ru(1)–Ru(2)	2.750(2)	C(1D)–C(2D)	1.531(5)
Ru(1)–Ru(3)	2.786(2)	C(1D)–C(8D)	1.528(5)
Ru(2)–Ru(3)	2.990(1)	C(2D)–C(3D)	1.519(5)
Ru(2)–H	1.76(2)	C(3D)–C(4D)	1.528(4)
Ru(3)–H	1.76(2)	C(4D)–C(5D)	1.371(5)
Ru(1)–C(4D)	2.280(3)	C(5D)–C(6D)	1.382(4)
Ru(1)–C(5D)	2.103(3)	C(6D)–C(7D)	1.510(5)
Ru(2)–C(4D)	2.053(3)	C(7D)–C(8D)	1.524(5)
Ru(3)–C(5D)	2.239(3)	Ru–C (CO) mean	1.920(4)
Ru(3)–C(6D)	2.373(3)	C–O (CO) mean	1.136(4)
C(8D)–C(1D)–C(2D)	118.0(3)	C(4D)–C(5D)–C(6D)	143.0(3)
C(1D)–C(2D)–C(3D)	114.6(3)	C(5D)–C(6D)–C(7D)	123.1(2)
C(2D)–C(3D)–C(4D)	113.9(3)	C(6D)–C(7D)–C(8D)	115.6(3)
C(3D)–C(4D)–C(5D)	120.2(3)	C(7D)–C(8D)–C(1D)	114.4(3)

Table 3 Calculated potential-energy values for hydride positions in molecules **1a** and **1b** as obtained from XHYDEX[5]

Hydride	Position	Potential energy/ kcal mol^{-1}
1	Ru(1)–Ru(2)	22.62
2	Ru(1)–Ru(2)	28.87
3	Ru(1)–Ru(3)	3.33
4	Ru(2)–Ru(3)	2.87
5	Ru(4)–Ru(5)	25.12
6	Ru(4)–Ru(5)	41.33
7	Ru(4)–Ru(6)	2.49
8	Ru(5)–Ru(6)	2.75
9	Ru(1)–Ru(2)–Ru(3)	3.02
10	Ru(4)–Ru(5)–Ru(6)	3.23

let in the hydride region indicating that the hydrides are fluxional over all possible positions.

It is also worth mentioning that the aliphatic chain in molecule **1a** is disordered: atoms C(14) and C(15) occupy two sites of occupancy 60 and 40% corresponding to two alternative foldings of the C_8 chain [see Fig. 1(*a*)]. With diffraction data collected at only one temperature, however, it is not possible to discriminate, based on diffraction data, between the static or dynamic nature of the disorder.

The organic moiety in compound **2** is bonded to the cluster in an allenylic fashion as shown in Fig. 2 and as first observed for a 1-methyl-3-ethyl-allenyl ligand bonded to a triruthenium cluster.[3] Although allenylic bonding to metal clusters has been previously characterized for linear systems, this compound represents the first example of a ring system exhibiting allenylic bonding to a cluster system. In **2** the allenylic angle C(4D)–C(5D)–C(6D) of 143.0(3)° is consistent with linear systems with similar bonding modes, and the bond lengths C(4D)–C(5D) 1.371(5) Å and C(5D)–C(6D) 1.382(4) Å are characteristic of olefinic bonds. The hydride atom was located on the Fourier map and is along the Ru(2)–Ru(3) edge, the bond length accordingly being the longest [2.990(1) Å]. The ruthenium–allenylic unit distances are in very close agreement with those in two previously characterized linear allenyl compounds, *viz*. $[Ru_3H(CO)_9(C_6H_9)]$[3] and $[Ru_3(CO)_9(C_6H_9)(PPh_2)]$[1b] (see Table 4), although the similarity is more evident between **2** and $[Ru_3H(CO)_9(C_6H_9)]$, as in the second example the bridging phosphido unit appears to affect the bond distances slightly. Thus, the C_8 ring can achieve the arrangement of linear allenyl systems with the resulting strain being accommodated by the relatively large unbonded section of the ring.

The co-ordination geometry of the carbonyls reflects the presence of the hydride ligands. In each case, they are 'pushed away' from the site of co-ordination of the hydride atoms. However, while the situation is not ambiguous for complex **2** (see Fig. 2), this is not so for **1** where the H ligands are disordered.

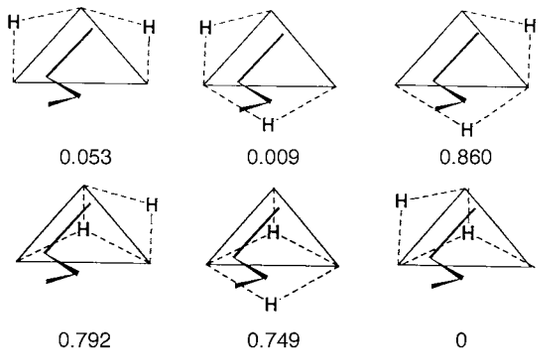

Scheme 1

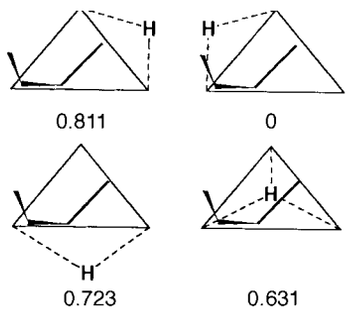

Scheme 2

In essence compound **2** can be generated from **1** *via* a hydride shift from the ruthenium cluster to C(7), however on heating **1** in octane **2** is formed along with three Ru_4 compounds, so no direct route has yet been found. Further investigations of this conversion are underway.

Molecular orbital calculations

Extended-Hückel molecular orbital calculations (see Experimental section for further details)[6] were performed for models of cluster **1**, $[Ru_3H_2(CO)_9(\mu_3\text{-}\eta^2\text{-}C_4H_4)]$, and of **2**, $[Ru_3H(CO)_9(\mu_3\text{-}\eta^3\text{-}C_4H_5]$, in order to find the positions of the hydride ligands and analyse the bonding mode of the organic ligands to $Ru_3H_x(CO)_9$. The cyclic ligand was modelled by a C_4H_4 or C_4H_5 chain of the appropriate topology to bind the cluster as observed in each structure.

Extended-Hückel calculations have been previously used in order to assign hydrides which could not otherwise be found. For instance, the preference for edge- or face-bridging hydrides in M_4 clusters has been discussed,[7] as well as the hydride position in simpler mononuclear bis(carbaborane)iron derivatives.[8]

The relative energies (eV) of the possible isomers of complex **1**, differing by the positions of the two hydrides, are given in Scheme 1. The Ru_3 cluster is seen from above and the dark line represents schematically the organic η^2 ligand in a position similar to the one occupied in the cluster. The hydride ligands can occupy two edge-bridging sites or one edge-bridging and one face-bridging site, as sketched. The asymmetry of the ligand is responsible for the non-equivalence of the edge-bridging sites. The most stable structure presents one face- and one edge-bridging hydride ligand, but some of the others have only slightly higher energies. This suggests that interconversion between different geometries may occur easily, consistent with experimental data. On the other hand, as the cluster framework was not optimized, these energies may in principle still be lowered, representing only a general trend.

In order to test the reliability of these results and have some calibration of the method, similar calculations were carried out for the second cluster, where the hydride position is known. As can be seen in Scheme 2 (relative energies in eV; the dark line shows the organic ligand in a schematic way), the fact that the

Table 4 Comparative analysis of bond lengths (Å) and angles (°) for complex **2**, and for the related cluster species $[Ru_3H(CO)_9(C_6H_9)]$[3] and $[Ru_3(CO)_9(C_6H_9)(PPh_2)]$[1b]

	2	$[Ru_3H(CO)_9(C_6H_9)]$	$[Ru_3(CO)_9(C_6H_9)(PPh_2)]$
Ru(1)–Ru(2)	2.750(2)	2.741(1)	2.6653(6)
Ru(1)–Ru(3)	2.786(2)	2.766(1)	2.8252(6)
Ru(2)–Ru(3)	2.990(1)	2.994(1)	3.0965(6)
Ru(1)–C(4D)	2.280(3)	2.261(5)	2.299(5)
Ru(1)–C(5D)	2.103(3)	2.089(5)	2.127(5)
Ru(2)–C(4D)	2.053(3)	2.058(5)	2.033(6)
Ru(3)–C(5D)	2.239(3)	2.242(5)	2.301(5)
Ru(3)–C(6D)	2.373(3)	2.341(6)	2.274(6)
C(4D)–C(5D)	1.371(5)	1.365(8)	1.352(8)
C(5D)–C(6D)	1.382(4)	1.368(10)	1.386(8)
C(4D)–C(5D)–C(6D)	143.0(3)	142.3(6)	143.7(3)

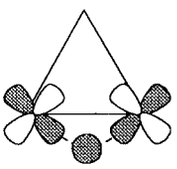

Scheme 3

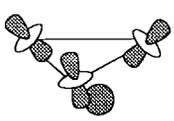

Scheme 4

carbonyl groups are not allowed to relax does not introduce significant repulsions when the hydride is moved around. The most stable isomer corresponds to the geometry experimentally observed (second from left).

Going back to the dihydride species, an examination of the bonding mode of each type of hydride for the most stable geometry was conducted. The hydride 1s orbital donates one electron pair to an empty symmetric combination of ruthenium orbitals. The metals use in-plane orbitals, which are almost only involved in metal–metal bonding to bind the hydride in the edge (Scheme 3, view from above).

The addition of the hydride does not greatly disturb the internal bonds of the cluster and that is why the edge-bridging hydrogen is more strongly bound than the facial one. The binding energies of each hydride to the rest of the cluster, defined as the difference between the sum of the energies of the isolated hydride and the $[Ru_3H(CO)_9(\mu_3\text{-}\eta^2\text{-}C_4H_4)]$ fragment and of the energy of the cluster, are, respectively, 2.25 (H_{edge}) and 1.59 eV (H_{face}). Positive binding energies mean attractive interactions. One special edge is favoured, because the presence of the ligand changes the metal orbitals in such a way that a better overlap is achieved in this case. On the other hand, the face-bridging hydrogen is below the ruthenium plane and the three metals must use orbitals which have components above and below that plane (Scheme 4). As they are also bonding relative to the organic ligand, the binding of the hydride weakens the Ru–C bonds.

The bonding of each organic ligand to the other fragment in the cluster will now be analysed. For the dihydride **1** the interaction is achieved by means of one C≡C bond. The diagram (Fig. 4) shows how the model $H_2C{=}CHC{\equiv}CH$ chain coordinates to Ru_3, donating electrons through its π orbitals ($\pi_\perp$ and $\pi_\parallel$, left side) and receiving electrons from the metal $d_{2\perp}$ in one of the empty π*($\pi^*_\perp$). As this chain folds up, enforced in the real molecule by the cyclic nature of the ligand, the interaction of the double bond with the metal atoms is negligible. In the end strong Ru–C bonds are formed, overlap populations being given in Scheme 5.

The allenyl cation in the monohydride cluster **2** has one H more than the ligand in **1** and can donate more electrons to the cluster. It has been studied from an organic chemistry point of view using *ab initio* calculations,[9] while its binding to triangular metal clusters was addressed using a different approach.[10] We therefore start by deriving the frontier orbitals of the twisted ligand, as it is observed in the cluster, from those of a linear species. The model is therefore a C_4H_5 chain, which can be

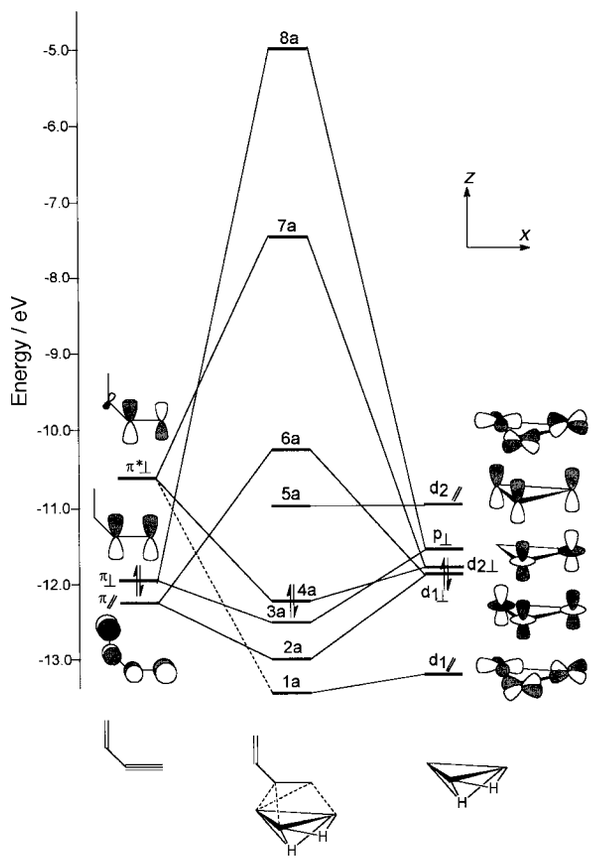

Fig. 4 Interaction diagram between $H_2C{=}CHC{\equiv}CH$ and $Ru_3H_2(CO)_9$ in the model of $Ru_3H_2(CO)_9(\mu_3\text{-}\eta^2\text{-}C_8H_{10})$] **1**

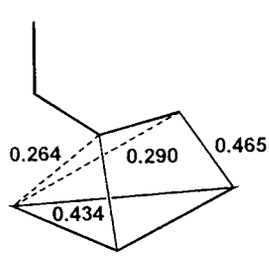

Scheme 5

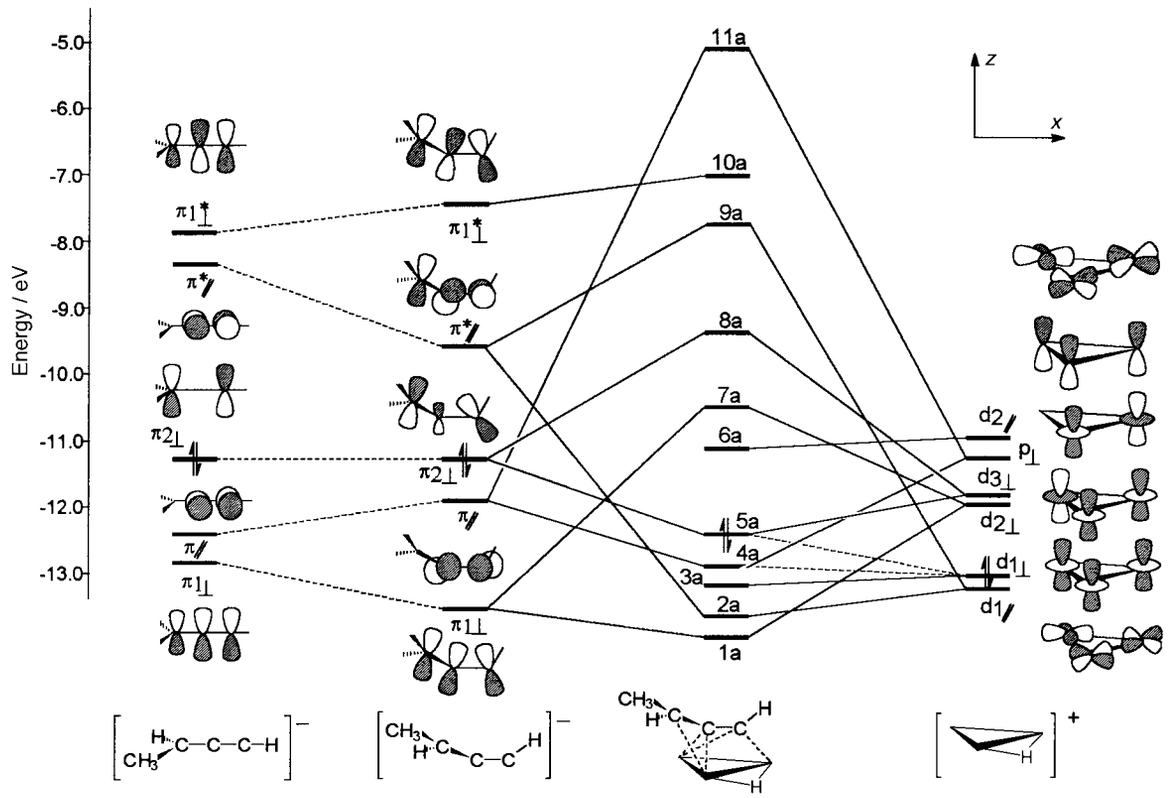

Fig. 5 Frontier orbitals of allenyl and the interaction diagram between the $HC{=}C{=}CH(CH_3)^-$ anion and $Ru_3H(CO)_9^+$ in the model of $[Ru_3H(CO)_9(\mu_3\text{-}\eta^3\text{-}C_8H_{11})]$ **2**

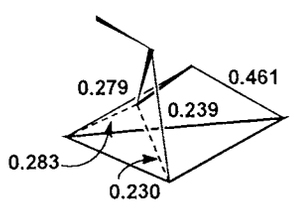

Scheme 6

described as $HC{=}C{=}CH(CH_3)^-$. This ligand can use the π bonds and the lone pair in the carbon atom and differs from a normal allenyl in the twisting of the chain, enforced by being part of a ring.

At the left-hand side of Fig. 5 are depicted the relevant orbitals of a linear allenyl ligand, which can easily be assigned as perpendicular or parallel π systems. They resemble those described in ref. 9, the absence of one C–H bond giving rise to a carbon lone pair (seen in the non-bonding allyl-type MO, $\pi_{2\perp}$). The distortion, caused by changing the C–C–C angle from 180 to 120°, and moving one carbon atom away from the initial plane of CCCH (as sketched in the lower part of the figure), leads to a mixing of σ and π character in the orbitals, but their main nature remains the same. The right-hand side of Fig. 5 shows the interaction between the distorted allenyl orbitals and those of the $Ru_3H(CO)_9$ fragment. It is very schematically drawn, as the final species has no symmetry and every orbital is allowed to mix. Essentially, there are three donation components, two from the C–C π bonds (through $\pi_{1\perp}$ and $\pi_{\parallel}$) and the third from the orbital concentrating the lone pair character ($\pi_{2\perp}$), which give rise to three formal Ru–C bonds. These are strengthened by a back-donation interaction from a combination of in-plane ruthenium orbitals ($d_{1\parallel}$) to $\pi^*_{\parallel}$. The metal–carbon overlap populations are given in Scheme 6. The main difference from Scheme 5 is the participation of the third carbon atom in binding to the ruthenium atoms. Both coordination modes lead to the formation of strong bonds, though their number is increased in cluster **2**.

Conclusion

Two isomers differing by one hydrogen, either co-ordinated to ruthenium or to carbon, were obtained from the same reaction. Though the two clusters have the same electron count, they carry different organic ligands. The allenyl ligand in complex **2** is observed in a new environment, σ and doubly π bonded to the triangular cluster core. Extended-Hückel calculations indicated that the two hydrides in **1** prefer to bridge over one edge and one face of the Ru_3 triangle, the preferred edge being the one parallel to the C≡C bond. While the possibility of interconversion between isomers was probed theoretically, no obvious low-energy pathway could be found. Most likely both isomers stem from a common intermediate which can evolve in multiple ways as the reaction proceeds.

Experimental

Synthesis and chemical characterization in solution

The reaction was carried out with the exclusion of air using solvents freshly distilled under an atmosphere of dry nitrogen. Further work-up of products was achieved without precautions to exclude air with standard laboratory-grade solvents. Infrared spectra were recorded on a Perkin-Elmer 1600 series FTIR spectrometer in CH_2Cl_2 using NaCl cells, positive fast atom bombardment mass spectra using a Kratos MS50TC spectrometer, with CsI as calibrant, and proton NMR spectra in $CDCl_3$ using a Bruker AM250 instrument, referenced to internal $SiMe_4$. Products were separated by thin-layer chromatograhy on plates supplied by Merck coated with a 0.25 mm layer of Kieselgel 60 F_{254}, using dichloromethane–hexane (30:70) as eluent. Trimethylamine *N*-oxide was obtained from Aldrich chemicals, as the dihydrate and sublimed immediately prior to reaction.

Thermolysis of $[Ru_3(CO)_{12}]$ (250 mg) in octane (25 cm^3) containing cycloocta-1,3-diene (five drops) for 4 h resulted in the formation of a deep red-brown solution. Removal of the solv-

Table 5 Crystal data and details of measurements for complexes **1** and **2***

	1	**2**
System	Triclinic	Monoclinic
Space group	$P\bar{1}$	$P2_1/n$
a/Å	9.526(8)	12.843(5)
b/Å	14.609(10)	10.109(4)
c/Å	16.797(9)	15.824(7)
α/°	66.39(3)	—
β/°	74.79(4)	99.58(8)
γ/°	87.92(4)	—
U/Å^3	2061(3)	2026(1)
D_c/g cm^{-3}	2.139	2.175
μ(Mo-Kα)/mm^{-1}	2.216	2.254
Octants explored, *hkl*	−10 to 11, −15 to 17, 0–20	−15 to 15, 0–12, 0–18
No. measured reflections	7401	5413
No. unique reflections used in the refinement	7231	3566
No. refined parameters	521	270
Goodness of fit on F^2	1.028	1.135
$R1$ [on F, $I > 2\sigma(I)$]	0.0635	0.0234
$wR2$ (on F^2, all data)	0.1779	0.1134

* Details in common: $C_7H_{12}O_9Ru_3$; M_r 663.48; $Z = 4$; $F(000)$ 1272; θ 2.5–25°. Weighting scheme: $w = 1/[\sigma^2(F_o^2) + (mP)^2 + nP]$, where $P = (F_o^2 + 2F_c^2)/3$ and $m = 0.1348$, $n = 6.7186$ for **1**; $m = 0.0305$, $n = 1.2377$ for **2**.

ent *in vacuo*, followed by thin-layer chromatography on silica using dichloromethane–hexane (1:4, v/v) as eluent, resulted in the isolation of several products. Compounds **1** and **2**, both yellow, were eluted first and second, respectively. Yields for both compounds were 8%. Elemental analysis and variable-temperature NMR data are not available. Spectroscopic data: **1**, IR ν_{CO}(hexane) 2104m, 2075s, 2052vs, 2039s and 2029s cm^{-1}; positive FAB mass spectrum *m/z* 665 (calc. 663); ^{1}H NMR ($CDCl_3$) δ 3.13 (t, 2 H), 2.55 (d, 2 H), 1.84 (s, 2 H), 1.65 (s, 4 H) and −18.06 (br, 2 H); **2**, IR ν_{CO}(hexane) 2091m, 2063s, 2037vs, 2020vs and 1997m cm^{-1}; positive FAB mass spectrum *m/z* 663 (calc. 663); ^{1}H NMR ($CDCl_3$) δ 3.72 (t, 1 H), 2.94 (m, 2 H), 2.45 (m, 1 H), 1.73 (m, 7 H) and −17.4 (s, 1 H).

Crystallography

X-Ray measurements were made at 150(2) K on a Stoë Stadi-4 four-circle diffractometer using Mo-Kα radiation (λ 0.710 73 Å). All relevant experimental details are in Table 5. An Oxford Cryosystems low-temperature device was used. Diffraction data were corrected for absorption by azimuthal scanning of high-χ reflections: minimum and maximum corrections 0.879 and 1.097 for complex **1**, and 0.885 and 1.092 for **2**. All non-H atoms in **1** were allowed to vibrate anisotropically, whereas in **2** only the ruthenium atoms were refined anisotropically. The H atoms in **1** and **2** were added in calculated positions and refined 'riding' on their respective C atoms. The low-temperature data collection for **2** could not prevent rapid decay under X-ray exposure (>40%), thus accounting for the limited data set and for the relatively low accuracy. The program SHELXS[11a] and SHELXL 93[11b] were used for data treatment and refinement based on F^2; SCHAKAL 93 was used for the graphical representation of the results.[11c]

Atomic coordinates, thermal parameters, and bond lengths and angles have been deposited at the Cambridge Crystallographic Data Centre (CCDC). See Instructions for Authors, *J. Chem. Soc., Dalton Trans.*, 1997, Issue 1. Any request to the CCDC for this material should quote the full literature citation and the reference number 186/295.

Molecular orbital calculations

All the molecular orbital calculations were done using the extended-Hückel method[6] with modified H_{ij} values.[12] The basis set for the metal atom consisted of *n*s, *n*p and (*n* − 1)d orbitals. The s and p orbitals were described by single Slater-type wavefunctions, and the d orbitals were taken as contracted linear combinations of two Slater-type wavefunctions. Standard parameters were used for H, C and O, while those for Ru were as follows (H_{ii}/eV, ζ): 5s, −10.40, 2.078; 5p, −6.89, 2.043; 4d, −14.90, 5.378, 2.303 (ζ_2), 0.5340 (C_1), 0.6365 (C_2).

All model geometries were based on the crystal structures. Pseudo-octahedral geometries were assumed around each Ru atom, with one axial and two equatorial carbonyl ligands, and all C (CO)–Ru–C (CO) set to 90°. The co-ordinating C–C bond in cluster **1** is parallel to the Ru_3 plane. For cluster **2** the angle between the plane defined by the three co-ordinating carbons and the Ru_3 triangle is 25°. In the organic ligands the aliphatic parts were replaced by hydrogen atoms, since the results were not qualitatively altered. A C_4 chain was thus used instead of a C_8 ring, with all internal angles analogous to those in the real clusters. The following distances (Å) were used: Ru–Ru 2.85, Ru–C (CO) 1.90, C–O 1.15, Ru–C 2.20, C–H 1.08, C–C 1.40 and Ru–H 1.80.

Acknowledgements

Financial support by the Ministero dell'Universita' e della Ricerca Scientifica e Tecnologica is acknowledged. B. F. G. J., D. B. and F. G thank NATO for a travel grant. The ERASMUS project 'Crystallography' is acknowledged for a student exchange (D. B. B.). D. B. B. and B. F. G. J. thank the EPSRC, ICI (Wilton). D. B., F. G., M. J. C. and L. F. V. acknowledge Consiglio Nazionale delle Ricerche (Italy) and Junta Nacional de Investigaçao Cientifica e Technológica (Portugal) for joint financial support.

References

1 (*a*) G. H. Young, A. Wojcicki, M. Galligaris, G. Nardin and N. Bresciani-Pahor, *J. Am. Chem. Soc.*, 1989, **111**, 6890; (*b*) G. H. Young, M. V. Parhael, A. Wojcicki, M. Galligaris, G. Nardin and N. Bresciani-Pahor, *Organometallics*, 1991, **10**, 1934.
2 D. Nucciarone, N. J. Taylor and A. J. Carty, *Organometallics*, 1984, **3**, 177; D. Nucciarone, S. A. MacLaughlin, N. J. Taylor and A. J. Carty, *Organometallics*, 1988, **7**, 106; J. Suades, F. Dahan and A. Mathieu, *Organometallics*, 1988, **7**, 47; C. E. Schuchart, A. Wojcicki, M. Calligaris, P. Faleschini and G. Nardin, *Organometallics*, 1994, **13**, 1999.
3 G. Gervasio, D. Osella and M. Valle, *Inorg. Chem.*, 1976, **15**, 1221.
4 M. I. Bruce, J. M. Guss, R. Mason, B. W. Skelton and A. H. White, *J. Organomet. Chem.*, 1983, **251**, 261; R. J. Goudsmit, B. F. G. Johnson, J. Lewis, P. R. Raithby and M. J. Rosales, *J. Chem. Soc., Dalton Trans.*, 1983, 2257; R. D. Adams, X. Qu and W. Wu, *Organometallics*, 1993, **12**, 4117; H. Chen, B. F. G. Johnson, J. Lewis and P. R. Raithby, *J. Organomet. Chem.*, 1989, **C7**, 376; R. D. Adams, G. Chen, X. Qu, W. Wu and J. H. Yamamoto, *J. Am. Chem. Soc.*, 1992, **114**, 10977.
5 A. G. Orpen, XHYDEX, A Program for Locating Hydrides, Bristol University, 1980; *J. Chem. Soc., Dalton Trans.*, 1980, 2509.
6 R. Hoffmann, *J. Chem. Phys.*, 1963, **39**, 1397; R. Hoffmann and W. N. Lipscomb, *J. Chem. Phys.*, 1962, **36**, 2179, 3489.
7 R. Hoffmann, B. E. R. Schilling, R. Bau, H. D. Kaesz and D. M. P. Mingos, *J. Am. Chem. Soc.*, 1978, **100**, 6088.
8 M. J. Calhorda and D. M. P. Mingos, *J. Organomet. Chem.*, 1982, **229**, 229.
9 H. Mayr and R. Schneider, *Chem. Ber.*, 1982, **115**, 3470.
10 G. Granozzi, E. Tondello, R. Bertoncello, S. Aime and D. Osella, *Inorg. Chem.*, 1985, **24**, 570.
11 (*a*) G. M. Sheldrick, *Acta Crystallogr., Sect. A*, 1990, **46**, 467; (*b*) G. M. Sheldrick, SHELXL 93, Program for Crystal Structure Determination, University of Göttingen, 1993; (*c*) E. Keller, SCHAKAL 93, University of Freiburg, 1993.
12 J. H. Ammeter, H.-B. Bürgi, J. C. Thibeault and R. Hoffmann, *J. Am. Chem. Soc.*, 1978, **100**, 3686.

Received 9*th July* 1996; *Paper* 6/04816A